2021 IEEE International Conference on Systems, Man, and Cybernetics (SMC)
17-20 October, 2021. Melbourne, Australia

An Extended Parameter Estimation Disturbance Observer for an Active Ankle Foot Orthosis

Benjamin DeBoer, Ali Hosseini, and Carlos Rossa

2021 IEEE International Conference on Systems, Man, and Cybernetics (SMC) | 978-1-6654-4207-7/21/$31.00 ©2021 IEEE | DOI: 10.1109/SMC52423.2021.9659241

***Abstract*— An active ankle foot orthosis (AAFO) is an assistive device that applies plantarflexion and dorsiflexion assistance to the ankle joint by means of a compliant actuator. The device must apply sufficient torque assistance to track the desired ankle trajectory. However, torque disturbances are prevalent throughout the gait cycle. Accurately modelling the AAFO in conjunction with the ankle joint disturbance torque is a difficult task, as the model parameters can change over time. As a result, parameters such as inertia and friction are often roughly estimated based on the user's weight. The uncertainties due to unmodelled disturbances and errors in dynamics modelling can severely compromise the device's ability to provide appropriate assistance.**

This paper presents a novel extended parameter estimation observer combined with a disturbance rejection controller to estimate the model's inertia and friction. First, an extended state observer (ESO) is employed in which the extended state is the estimated disturbance. Knowing the nominal ankle torque trajectory and the disturbance, a novel control law is formulated to reject the effects of endogenous disturbance torque during trajectory tracking. Then, based on the observed difference between the observed disturbance and nominal ankle torque, the paper introduces a novel method to estimate the inertial and friction parameters of the AAFO.

Simulation results show that state feedback with the ESO is able to reduce the root mean square tracking error by 5.2% and 71.1% for high and low feedback gains, respectively. The results also indicate that the estimated AAFO and ankle joint inertial and damping parameters converge close to the nominal plant parameters. Simulations also show the effectiveness of the estimation laws from various initial plant estimates.

I. Introduction

An ankle foot orthosis (AFO) is commonly a passive device used to assist patients who have little to no dorsiflexion capability, known as foot drop. Foot drop can be a result of stroke, cerebral palsy, or multiple sceloris. AFOs are employed to limit the dorsiflexion and plantarflexion range of the ankle joint, eliminating the chance of the toe contacting the ground when the foot is in the swing phase. The goal of an active AFO (AAFO) is to track the nominal angular trajectory of the ankle joint using assistive methods. The most common actuation method involves the use of a series elastic or variable impedance actuator [1], [2].

It is well-known that ankle trajectory tracking is subjected to highly non-linear disturbance torques of large magnitudes. Additionally, the plant parameters of the AAFO in combination with the ankle cannot be directly measured, resulting in increased disturbances in the form of modelling uncertainties. Previous research has been focused on rejecting the disturbance torque by means of observers or adaptive control laws to track a trajectory [3]–[7]. However, there has been little focus on reducing the error in the modelled plant parameters.

To model the AAFO disturbance, two methods have been explored. Kirtas *et al.*, modelled the disturbances as the summation of a number of sine waves at various frequencies, phase shifts, and scales [8]. The modelled disturbance is used in an adaptive backstepping controller for an AAFO in which the plant parameters are known, reducing the Root Mean Square (RMS) tracking error and maximum overshoot. Huo *et al.* modelled the disturbance torque using a sum of dynamic torques, including: frictional, inertial, stiffness, ground reaction, gravitational, user, and actuator [4]. The formulations of each dynamic torque required an estimated scaling factor to correctly model the theoretical disturbance torque. To estimate these factors, Arnez *et al.* developed an adaptive controller based on the s-plane principle of Slide Mode Control (SMC), subtracting the modelled disturbance torque from the control signal of a proportional or proportional-derivative controller to reduce the tracking error [3], [4].

To avoid modelling the disturbance, which is impossible to completely model due to variations in individual steps, previous works have used extended state observers (ESO) to reject the total system disturbance. The application of an ESO in an AAFO's and ankle exoskeletons have been explored by [5] and [6], respectively, using active disturbance rejection control to eliminate exogenous (standard disturbance) and endogenous (unmodelled dynamics) torque disturbances throughout the gait cycle. Guerrero *et al.* utilized a trajectory tracking controller to follow a predefined trajectory which was tested on healthy subjects where low assistive torque values were measured and rejected [5]. Since, Zhao *et al.*, implemented SMC with an ESO in order to minimize the chattering effect of SMC in the presence of disturbances while actuating an ankle exoskeleton [9]. The work analyzed the stability and magnitude of the ESO, and proved to reduce the torque tracking error when used on test subjects.

While disturbance rejection has been studied to a great extent, the identification of the model parameters of AAFOs have been limited, as the majority of the endogenous torque disturbances are absorbed by adaptive controllers. For example, Bagheri *et al.* used adaptive SMC to account for the error in the dynamic model of the AAFO [7]. The experiment tracked a desired force within a series elastic actuator while adapting to the inertial, stiffness, and damping parameters of the actuator. In previous works the parameters of the

Faculty of Engineering and Applied Science, Ontario Tech University, Oshawa, Ontario, Canada. Email: benjamin.deboer@ontariotechu.ca; sayyedali.hosseini@ontariotechu.ca; rossa@sce.carleton.ca

modelled plant were consistently estimated and invariant in time. However, the inertial, damping, and energy storage parameters of the AAFO combined with the ankle joint are not measurable and therefore an estimation law of the plant parameters can be developed.

This paper presents an novel model parameter estimation law focused on reducing the endogenous disturbance torque within the system. An ESO is employed to identify and reject the total disturbance to the AAFO, where the estimation law is based on the difference between a nominal ankle torque trajectory and the identified torque by the ESO. The resulting estimation law allows the estimated model parameters of the AAFO to converge to the plant parameters, facilitating future application of adaptive model based control.

The paper is structured in the following manner. Sec. II introduces a dynamic model of the AAFO, which is then used in Sec. III to derive the proposed control system. Sec. IV further uses the model and controller to establish the novel estimation law. Simulations of the proposed controller in Sec. V demonstrated the effectiveness of the proposed approach to identify the model parameters while rejecting torque disturbances. Further considerations and conclusion follow in Sec. VI and VII, respectively. Overall, the novel estimation laws are capable of minimizing the endogenous disturbance torque by reducing the error in the dynamics modelling.

II. Ankle Foot Orthosis Model

The dynamic model of an AAFO can be expressed as:

$$J\ddot{\theta} + B\dot{\theta} + K\theta = \tau_d + \tau_a \tag{1}$$

where J is the rotational inertia of the AAFO and ankle joint, B is the viscous damping coefficient, K is the stiffness coefficient, τ_d is the disturbance torque, τ_a is the torque applied by the actuator, θ is the ankle joint angle, and static friction is assumed to be negligible. The state space representation of the model is:

$$\begin{bmatrix}\dot{\theta}_1\\ \dot{\theta}_2\end{bmatrix} = \underbrace{\begin{bmatrix}0 & 1\\ -\frac{K}{J} & -\frac{B}{J}\end{bmatrix}}_{A}\begin{bmatrix}\theta_1\\ \theta_2\end{bmatrix} + \underbrace{\begin{bmatrix}0\\ \frac{1}{J}\end{bmatrix}}_{B}(\tau_d + \tau_a)$$

$$y = \underbrace{\begin{bmatrix}1 & 0\end{bmatrix}}_{C}\begin{bmatrix}\theta_1\\ \theta_2\end{bmatrix}$$

where $\theta_1 = \theta$, $\theta_2 = \dot{\theta}$. The nominal gait angular and torque trajectory of an individual without foot drop is shown in Fig. 1, in which the main goal of an AAFO control system is to track the angular trajectory. The torque developed at the ankle joint can be treated as the combined disturbance (τ_d) to the AAFO, measured by [10] with the aid of force plates and motion capture equipment. In the case the user has partial to full muscle activation, the disturbance to the system is scaled down. To correctly track the angular trajectory, the large torque disturbance must be identified and compensated by means of a robust control system.

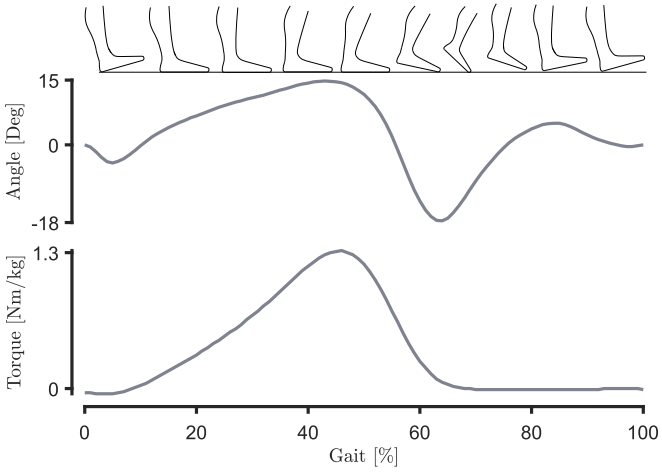

Fig. 1. Nominal gait data for a healthy adult with an average gait time of 1.1 seconds. Data retrieved from [10]. The applied torque is normalized by the individual's mass.

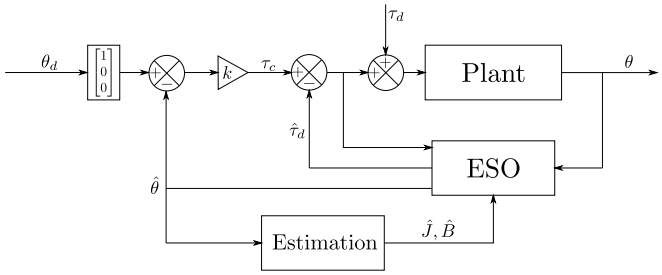

Fig. 2. Control system topology. θ_d is the desire trajectory, θ is the plant output, τ_d is the disturbance, $\hat{\tau_d}$ is the estimated disturbance, and k is the state feedback gain to eliminate tracking error.

III. Disturbance rejection for trajectory tracking

The proposed AAFO control system, as shown in Fig. 2 is comprised of the AAFO device (plant), the ESO, a state feedback controller, and relies on the estimation of the plants J and B parameters. In this work the stiffness coefficient (K) is assumed to be negligible based on various mechanical designs of AAFO's. The ESO is implemented to concurrently reject the effects of external disturbances and unmodelled dynamics. Based on the identified torque disturbance and the nominal torque at the ankle joint, the plant parameters B and J are estimated to minimize modelling errors.

A. State Feedback Controller

To eliminate the trajectory tracking error of the AAFO, state feedback is applied to the system. The AAFO model, similar to a standard spring damper control system, is known to be controllable by state feedback methods. Selecting state feedback gains (k) can be done by manual pole placement. While state feedback is efficient at minimizing tracking error the output deteriorates in the presence of large disturbances, therefore the implementation of the ESO will provide better tracking capability.

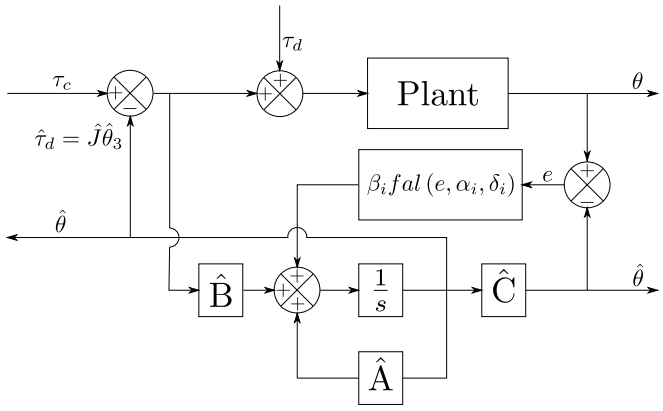

Fig. 3. Non-Linear ESO Topology in which the disturbance rejection torque is the estimated extended stated (θ_3) times the estimated inertia ($\hat{J}$).

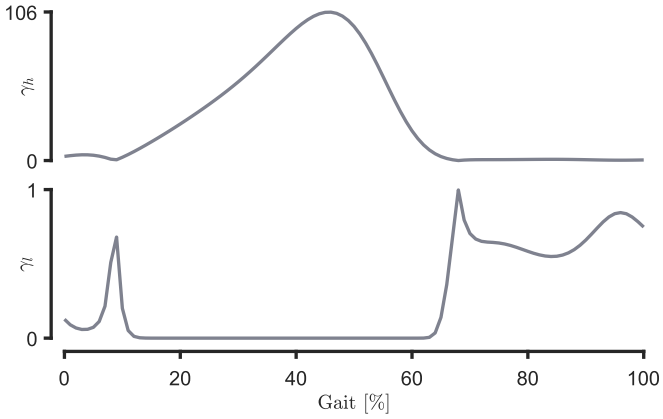

Fig. 4. Gain value with respect to the gait cycle for instances of estimation at high (γ_h) and low (γ_l) disturbance instances, where $\zeta = 2$ and $\alpha = 1$ in (6) based on a 80 kg user.

B. Extended State Observer

A linear state observer estimates the current plant states based on the difference between the plant output and modelled output define as [11].

$$\dot{\hat{x}} = A\hat{x} + Bu + LC(y - \hat{y}) \tag{2}$$

where A, B, and C are the modelled plant parameters and L, y, $\hat{y}$ is the observer gain, plant output, and observer output, respectively. However, when an unknown disturbance is applied to the system, the observer state estimates do not match the plant. Therefore, the ESO is designed to approximate the disturbances of the system using an additional extended state. The error between desired (θ_d) and actual (θ) ankle position can be controlled through the applied torque. By adding an extended state to the system, i.e., $\ddot{\theta}$, the value of the state is used as an additional control effort to reject disturbances. The ESO is expressed as

$$\begin{cases} \dot{\hat{\theta}}_1 = \hat{\theta}_2 + \beta_1 fal\,(e, \alpha_1, \delta_1) \\ \dot{\hat{\theta}}_2 = \hat{\theta}_3 + \frac{\tau_c - \hat{\tau}_d - \hat{B}\hat{\theta}_2}{\hat{J}} + \beta_2 fal\,(e, \alpha_2, \delta_1) \\ \dot{\hat{\theta}}_3 = \beta_3 fal\,(e, \alpha_3, \delta_3) \end{cases} \tag{3}$$

where $fal\,(e, \alpha_i, \delta_i)$ is a non-linear gain function defined by [12], for $i = 1, \ldots, n$ where n is the number of states. The scalar values of β_i are selected by poles placement or optimization, such as works in [13]. The non-linear gain function is evaluated as [12]:

$$fal\,(e, \alpha_i, \delta_i) = \begin{cases} |e|^{\alpha_i} \text{sign}(e) & |e| > \delta_i \\ \frac{e}{\delta_i^{1-\alpha_i}} & |e| \leq \delta_i \end{cases} \tag{4}$$

where $\delta_i > 0$, $\alpha_i > 0$, and $e = \theta - \hat{\theta}$. For the torque controlled system, the respective value of $\hat{\tau_d} = \hat{\theta}_3 \hat{J}$ is added to the control signal τ_c, to compensate for the disturbances (τ_d), as shown in Fig. 3.

To ensure observablility of the AAFO ESO system, the observability matrix is defined as:

$$Obs = \begin{bmatrix} C & CA & CA^2 \end{bmatrix}^T$$

where

$$A = \begin{bmatrix} 0 & 1 & 0 \\ 0 & 0 & 1 \\ 0 & 0 & 0 \end{bmatrix}, C = \begin{bmatrix} 1 & 0 & 0 \end{bmatrix}$$

which leads to

$$Obs = \begin{bmatrix} 1 & 0 & 0 \\ 0 & 1 & 0 \\ 0 & 0 & 1 \end{bmatrix}$$

Since the observability matrix is full rank, the system is observable and thus an ESO can be used for disturbance rejection.

IV. Parameter Estimation

Based on the difference between the extended state observed disturbance and nominal ankle torque disturbance, this section introduces a novel method to estimate the inertial J and friction B parameters of the AAFO. Guerrero *et al.* state that the exact rotational inertia of the users foot cannot be measured directly, and therefore a constant inertial value is used in their model based on standardized foot weight and centre of mass [5].

In order to determine J and B using online estimation, the known cyclic disturbance trajectory can be referenced, see Fig. 1. Instances with large disturbances are insufficient in determining the plant parameters but lower disturbance levels can be used to estimate parameters by referencing the ESO torque output and the nominal torque disturbance. The goal of the estimation law is to identify the parameters B and J such that the disturbance calculated through the ESO converges to a known nominal disturbance torque, which is based on the weight and applied assistance of the user. Two gain functions are used in the parameter estimation, where gain

$$\gamma_h = ||\alpha \tau_{Nom}|| \tag{5}$$

is used for estimating parameters that have a greater effect on the disturbance when the magnitude of the disturbance

is large. The desired estimates at low disturbances are governed by:

$$\gamma_l = \frac{1}{\zeta^{||\alpha\tau_{Nom}||}} \tag{6}$$

where $\zeta > 1$ is a scalar that penalizes larger instance of the nominal disturbance, see Fig. 4. Since parameter estimation is based on the difference between the nominal torque τ_d and rejected torque $\hat{\tau_d}$, the rejected torque from the ESO must be scaled so that the magnitude matches that of the users nominal torque. The scaling constant also needs to be estimated. In the case of the AAFO, the user may not require the full torque in relation to their mass. Therefore, the scale of the rejected torque (α) used for comparison is updated based on the difference between the peak instances of nominal torque in the gait cycle as:

$$\dot{\alpha} = a_\alpha \gamma_h \underbrace{\left(\tau_{Nom} + \alpha \cdot \hat{\theta}_3 \hat{J}\right)}_{\text{disturbance error}} \alpha \tag{7}$$

where γ_h is selected as the gain function, and $a_\alpha > 0$ is a scalar gain modified to optimize convergence. Comparing the nominal torque disturbance with the scaled ESO measured disturbance, the disturbance due to the unmodelled dynamics can be exposed. The endogenous torque due to error in the plant modeling is:

$$\tau_{d-model} = \left(J - \hat{J}\right)\ddot{\theta} + \left(B - \hat{B}\right)\dot{\theta} \tag{8}$$

where $\hat{J}$ and $\hat{B}$ are the estimated model parameters. Therefore, by analyzing the error dynamics the estimate of the inertial parameter J can be determined by:

$$\dot{\hat{J}} = -a_J \gamma_l \underbrace{\left(\tau_{Nom} + \alpha \cdot \hat{\theta}_3 \hat{J}\right)}_{\text{disturbance error}} \cdot \hat{J} \tag{9}$$

where $a_J > 0$ is the inertial scaling factor. Since the disturbance torque for damping is a function of $\dot{\theta}$, the estimate of B is updated as:

$$\dot{\hat{B}} = -a_B \gamma_l \hat{\theta}_2 \underbrace{\left(\tau_{Nom} + \alpha \cdot \hat{\theta}_3 \hat{J}\right)}_{\text{disturbance error}} \hat{B} \tag{10}$$

where $\hat{\theta}_2$ is the observed $\dot{\theta}$ of the AAFO, and $a_B > 0$ is the scalar gain. It is noted that the disturbance torque due to the error between J and $\hat{J}$ depends on $\ddot{\theta}$, however the use of the observed value, which is the extended state, would not lead to convergence as the disturbance error is based on the same state.

Since the estimation law of J and B depend on the same disturbance error, their convergence is dependant on one another. Regardless of the values of the scalar gains a_α, a_J, a_B, the proposed method can converge to the true value of J and B based on the endogenous torque disturbance relationship presented in (8).

V. Simulation

To prove the effectiveness of the control system and novel estimation law presented in Sec. III, simulations are conducted in MATLAB using embedded differential solvers. Gait data for the ankle joint is retrieved from the study presented in [10], consisting of the reference ankle trajectory and nominal ankle torque (Fig. 1). The simulations of the control system first analyzes the advantages of the ESO in comparison to direct state feedback, followed by the implementation of the plant parameter estimation. The simulations are conducted based on a 80 kg user with an nominal gait time of 1.1 seconds as presented in [10].

A. Extended State Observer

To identify the advantages of ESO for disturbance rejection, simulations are conducted using state feedback, and state feedback in combination with the ESO. The desired torque output of the actuator τ_a is a function of state feedback and the ESO rejected disturbance torque. The state feedback gain was determined by placing poles at $[-100, -100]$ for $[\theta, \dot{\theta}]$ resulting in the feedback gain:

$$k = \begin{bmatrix} 10000 & 200 \end{bmatrix} \tag{11}$$

where the control effort τ_c is determined by:

$$\tau_a = \tau_c = k \begin{bmatrix} \theta_d - \theta_1 \\ -\theta_2 \end{bmatrix} \tag{12}$$

In the above, θ_1, θ_2 are the current states of the AAFO, and θ_d is the desired angular position at the particular time instance. It is assumed that full state measurement of the ankle joint is available for stand alone state feedback control. Combining the state feedback controller with an ESO, the controller gains are modified to:

$$k = \begin{bmatrix} 10000 & 200 & 0 \end{bmatrix} \tag{13}$$

and thus the controller output is determined by

$$\tau_c = k \begin{bmatrix} \theta_d - \hat{\theta}_1 \\ -\hat{\theta}_2 \\ -\hat{\theta}_3 \end{bmatrix} \tag{14}$$

where $\hat{\theta}_1, \hat{\theta}_2, \hat{\theta}_3$ are the observed states. The control signal passed to the plant is the sum of the controller and disturbance rejection torque as

$$\tau_a = \tau_c - J_0 \hat{\theta}_3 \tag{15}$$

in which $J_0 = J$ if known, else $J_0 = \hat{J}$ is substituted. To determine the non-linear observer gains the scalar values $\beta_1, \beta_2, \beta_3$ where determined by pole placement of a linear observer at $[-100, -100, -100]$. The respective values of $\alpha_1, \alpha_2, \alpha_3$ were retrieved from [12] and the values of $\delta_1, \delta_2, \delta_3$ were determined experimentally as 0.001. Therefore, the non-linear observer gain is expressed as:

$$L = \begin{bmatrix} 3 \cdot 10^2 \cdot fal\left(\tilde{\theta}, 1.00, 0.001\right) \\ 3 \cdot 10^4 \cdot fal\left(\tilde{\theta}, 0.50, 0.001\right) \\ 1 \cdot 10^6 \cdot fal\left(\tilde{\theta}, 0.25, 0.001\right) \end{bmatrix} \tag{16}$$

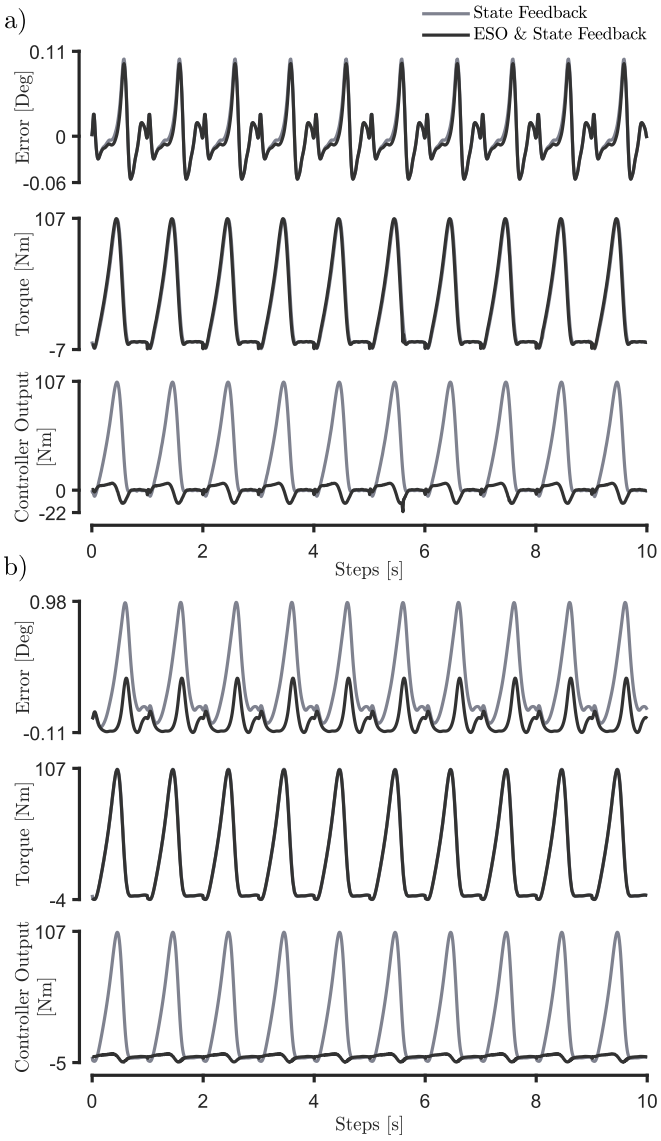

Fig. 5. Tracking and control comparison results between state feedback and state feedback in combination with ESO. a) High controller gains b) Low controller gains. The error corresponds to the difference between the desired angular trajectory and AAFO angular position.

The result of implementing the stand alone state feedback controller and the combination of state feedback control and ESO is shown in Fig. 5a. The state feedback controller is able to track the required angular trajectory of the system, with only a 0.035 deg RMS error between the desired angular trajectory and plant output, applying a control signal similar to the nominal disturbance torque. However, in combination with the ESO the RMS tracking error is reduced to 0.033 deg, while applying a higher assistive torque.

The tracking capability of the stand alone state feedback controller is linked to the high controller gains. In the presence of low controller gains such as:

$$k = \begin{bmatrix} 100 & 20 & 0 \end{bmatrix}$$

the RMS tracking error of the state feedback controller increases significantly to 0.421 deg in comparison with the combined system of only 0.122 deg, see Fig. 5b.

B. Parameter Estimation

To test the novel parameter estimation, simulations with a large and small initial estimate of both J and B with the static plant parameters of $J = 0.03$ and $B = 0.02$ are conducted. The estimation gain scalars a_α, a_J, a_B are set to $5 \cdot 10^{-4}$, 5, and 5, respectively. A filter, first order with a time constant of 2 seconds, was applied to the estimates of J and B to allow the system to operate with parameter values of low variance for each gait cycle. The results are shown in Fig. 6a, where the raw and filtered parameter estimation can be seen in Fig. 6b for two test cases. It is evident in the simulations that the system converges close to the real plant parameters, indicated by the straight dashed lines in Fig. 6. To analyze the effects of a reduced nominal torque on parameter convergence, two test cases were evaluated where only 50% of the nominal disturbance was applied. The results, see Fig. 6c, shows the quick convergence of α and the minimal effect of α on converging $\hat{J}$ and $\hat{B}$ to the real plant values. Therefore, the estimation laws are efficient at determining the plant parameters of the AAFO.

VI. Results & Discussion

The novel parameter estimation law presented in this work shows the feasibility of identifying and minimizing endogenous disturbance torques. The result is a system that converges to the real plant parameters, over a significant number of steps.

In an effort to analyze the effects of the estimation gains a_J and a_B, their values are sampled with the convergence based on number of steps to achieve a 5% settling time, in relation to the final parameter value. The results, see Table. I, express that for convergence the optimal gain values are $a_J = 5, a_B = 20$, using a first order filter with a time constant of 5 seconds. The data shows that further increasing $a_J > 5$ increases the settling time of J due to transient in convergence. Additionally, it is noted that regardless of the gains a_B and a_J, the damping parameter is the last to convergence.

The proposed estimation law is beneficial for AAFO optimal and adaptive control schemes such as SMC, Adaptive Backstepping, and Model Predictive Control (MPC). These controllers require an accurate model of the plant parameters in order to determine the best control signal. In combination with an ESO, the control systems only need to determine the control effort based on the plant parameters, where errors in the plant model will skew the performance of the controller. The implementation of the novel parameter estimation and disturbance rejection allows the controller to solely focus on the minimization of the tracking error.

VII. Conclusion

The control system proposed in this paper is efficient at identifying and rejecting unknown disturbances to an AAFO, while estimating the plant's inertial and damping parameter. The novel plant parameter estimation law, based

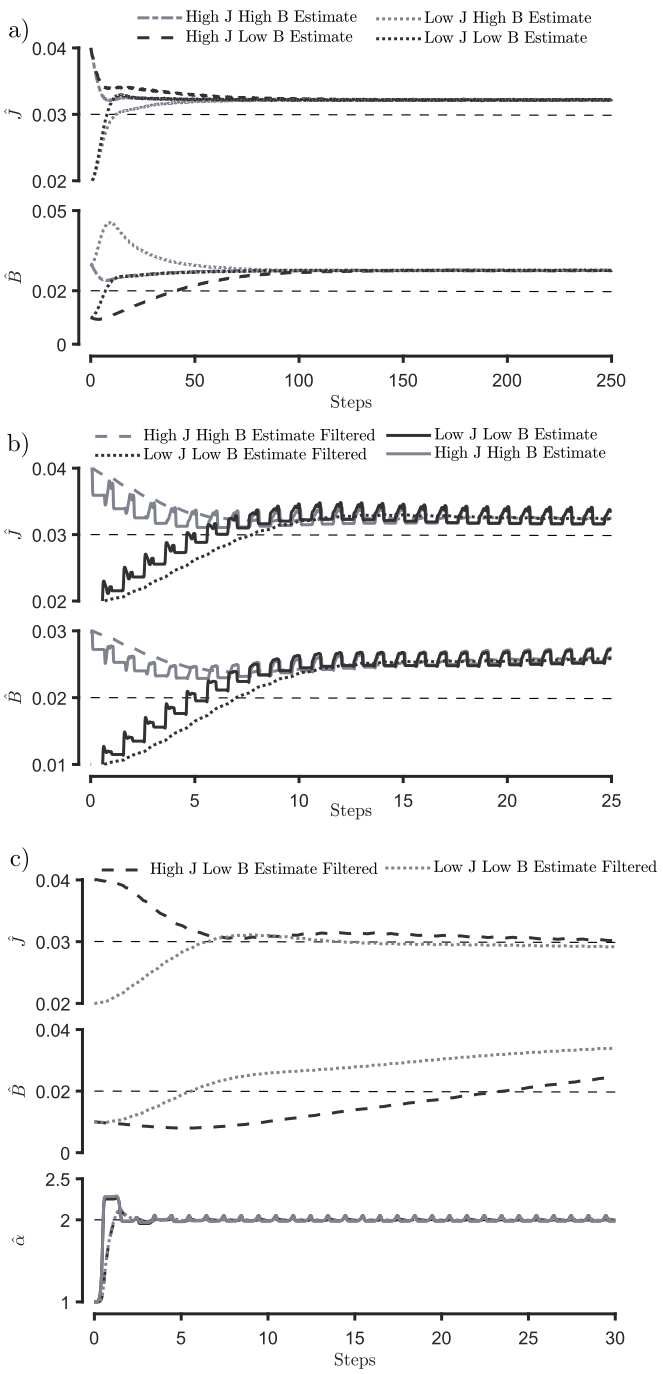

Fig. 6. a) Filtered parameter estimation results of high and low parameter estimates. b) Raw and filtered parameter estimation results of two estimates. c) Filtered parameter estimation and α estimation for a 50% disturbance torque. Where the straight dashed lines represent the real plant parameters.

TABLE I

PARAMETER SETTLING TIME [ST] PER ESTIMATION SCALAR

a_J	5	5	5	10	10	10	15	15	15
a_B	15	20	25	35	40	45	30	35	40
J ST [Steps]	9	9	5	5	5	5	3	3	3
B ST [Steps]	33	20	29	28	28	34	26	24	32

on identifying and correcting the error in dynamics modelling, is capable of converging to the real plant parameters of the AAFO under various initial conditions. The ESO proved effective in accurately determining and rejecting any disturbances injected into the system. The observer is able to reduce the RMS tracking errors by 5.2% and 71.1% in the presence of high and low feedback gains, respectively. The estimation of the plant parameters, although not required for state feedback control, will prove effective in future non-linear and optimal controllers for AAFO's.

Future work will focus on replacing the state feedback controller with a non-linear MPC controller, as current AAFO actuators are subject to non-linear torque and speed constraints. Future testing will target the efficacy of the adaptive observer in the presence of noise and disturbance.

REFERENCES

[1] K. W. Hollander, R. Ilg, T. G. Sugar, and D. Herring, "An efficient robotic tendon for gait assistance," 2006.

[2] M. Moltedo, T. Bacek, K. Junius, B. Vanderborght, and D. Lefeber, "Mechanical design of a lightweight compliant and adaptable active ankle foot orthosis," in *2016 6th IEEE International Conference on Biomedical Robotics and Biomechatronics (BioRob)*. IEEE, 2016, pp. 1224–1229.

[3] V. Arnez-Paniagua, H. Rifaï, Y. Amirat, S. Mohammed, M. Ghedira, and J.-M. Gracies, "Modified adaptive control of an actuated ankle foot orthosis to assist paretic patients," in *2018 IEEE/RSJ International Conference on Intelligent Robots and Systems (IROS)*. IEEE, 2018, pp. 2311–2317.

[4] V. Arnez-Paniagua, H. Rifaï, Y. Amirat, M. Ghedira, J. Gracies, and S. Mohammed, "Adaptive control of an actuated ankle foot orthosis for paretic patients," *Control Engineering Practice*, vol. 90, pp. 207–220, 2019.

[5] J. Guerrero-Castellanos, H. Rifaï, V. Arnez-Paniagua, J. Linares-Flores, L. Saynes-Torres, and S. Mohammed, "Robust active disturbance rejection control via control lyapunov functions: Application to actuated-ankle–foot-orthosis," *Control Engineering Practice*, vol. 80, pp. 49–60, 2018.

[6] Y. Long, Z. Du, L. Cong, W. Wang, Z. Zhang, and W. Dong, "Active disturbance rejection control based human gait tracking for lower extremity rehabilitation exoskeleton," *ISA transactions*, vol. 67, pp. 389–397, 2017.

[7] A. Bagheri, D. Dorostkar, M. R. Zakerzadeh, M. J. Sadigh, and M. Mahjoob, "Assessment of the adaptive sliding mode control of an active ankle foot orthosis with an impedance reference," in *2019 7th International Conference on Robotics and Mechatronics (ICRoM)*. IEEE, 2019, pp. 503–507.

[8] O. Kirtas, Y. Savas, M. Bayraker, F. Baskaya, H. Basturk, and E. Samur, "Design, implementation, and evaluation of a backstepping control algorithm for an active ankle–foot orthosis," *Control Engineering Practice*, vol. 106, p. 104667, 2021.

[9] J. Zhao, T. Yang, X. Sun, J. Dong, Z. Wang, and C. Yang, "Sliding mode control combined with extended state observer for an ankle exoskeleton driven by electrical motor," *Mechatronics*, vol. 76, p. 102554, 2021.

[10] G. Bovi, M. Rabuffetti, P. Mazzoleni, and M. Ferrarin, "A multiple-task gait analysis approach: kinematic, kinetic and emg reference data for healthy young and adult subjects," *Gait & posture*, vol. 33, no. 1, pp. 6–13, 2011.

[11] S. E. Talole, J. P. Kolhe, and S. B. Phadke, "Extended-state-observer-based control of flexible-joint system with experimental validation," *IEEE Transactions on Industrial Electronics*, vol. 57, no. 4, pp. 1411–1419, 2009.

[12] J. Han, "From pid to active disturbance rejection control," *IEEE transactions on Industrial Electronics*, vol. 56, no. 3, pp. 900–906, 2009.

[13] B. DeBoon, S. Nokleby, and C. Rossa, "Multi-objective gain optimizer for a multi-input active disturbance rejection controller: Application to series elastic actuators," *Control Engineering Practice*, vol. 109, p. 104733, 2021.